Neoplasia • Vol. 7, No. 1, January 2005, pp. 57–66

www.neoplasia.com

Host Plasminogen Activator Inhibitor-1 Promotes Human Skin Carcinoma Progression in a Stage-Dependent Manner[1]

Catherine Maillard, Maud Jost*, Maria Unni Rømer†, Nils Brunner†, Xavier Houard*, Annabelle Lejeune*, Carine Munaut*, Khalid Bajou*, Laurence Melen*, Keld Dano†, Peter Carmeliet‡, Norbert E. Fusenig§, Jean Michel Foidart* and Agnès Noel**

*Laboratory of Tumor and Development Biology, CRCE, CBIG, University of Liège, Tour de Pathologie (B23), Sart Tilman, Liège B-4000, Belgium; †Finsen Laboratory, Rigshospitalet, Strandboulevarden 49, Copenhagen DK 2100, Denmark; ‡Center for Transgene Technology and Gene Therapy, Flanders Interuniversity Institute for Biotechnology, KU Leuven, Leuven B-3000, Belgium; §Division of Carcinogenesis and Differentiation, German Cancer Research Center (DKFZ), Im Neuenheimer Feld 280, Heidelberg 69120, Germany

Abstract

Angiogenesis and tumor expansion are associated with extracellular matrix remodeling and involve various proteases such as the plasminogen (Plg)/plasminogen activator (PA) system. Recently, several experimental data have implicated the plasminogen activator inhibitor-1 (PAI-1) in tumor angiogenesis in murine systems. However, little is known about PAI-1 functions in human skin carcinoma progression. By generating immunodeficient mice (in Rag-1$^{-/-}$ or nude background) deleted for *PAI-1* gene (*PAI-1*$^{-/-}$), we have evaluated the impact of host PAI-1 deficiency on the tumorigenicity of two malignant human skin keratinocyte cell lines HaCaT II-4 and HaCaT A5-RT3 forming low-grade and high-grade carcinomas, respectively. When using the surface transplantation model, angiogenesis and tumor invasion of these two cell lines are strongly reduced in PAI-1–deficient mice as compared to the wild-type control animals. After subcutaneous injection in PAI-1$^{-/-}$ mice, the tumor incidence is reduced for HaCaT II-4 cells, but not for those formed by HaCaT A5-RT3 cells. These data indicate that PAI-1 produced by host cells is an important contributor to earlier stages of human skin carcinoma progression. It exerts its tumor-promoting effect in a tumor stage–dependent manner, but PAI-1 deficiency is not sufficient to prevent neoplastic growth of aggressive tumors of the human skin.

Neoplasia (2005) **7**, 57–66

Keywords: PAI-1, cancer invasion, tumoral angiogenesis, serine protease, protease inhibitor.

Introduction

The plasminogen (Plg)/plasminogen activator (PA) system has been implicated in tissue remodelings associated with both physiological and pathologic processes such as wound healing, mammary gland involution, angiogenesis, and cancer invasion. Serine proteases of the PA system are produced both by stromal and neoplastic cells [1,2]. The PA system is composed of several protein members: 1) Plg, an inactive proenzyme; 2) urokinase PA (uPA) and 3) tissue-type PA (tPA), two serine proteinases able to convert Plg into plasmin; 4) uPA receptor (uPAR); and 5) plasminogen activator inhibitors type I and type II (PAI-1 and PAI-2). These extracellular proteases have multiple functions. Besides their roles in extracellular matrix (ECM) degradation and remodeling, they may also influence the degradation and/or bioavailability of chemokines, cytokines, or their receptors [3–5]. PAI-1 is a multifunctional glycoprotein containing two active segments. One segment controls matrix proteolysis by inhibiting the conversion of Plg into plasmin by uPA and tPA. The other segment plays a role during cellular adhesion and migration by blocking interaction between vitronectin and different cell surface–associated molecules such as uPA/uPAR complex and integrins (for review, see Refs. [6,7]).

Based on extensive clinical and experimental studies, the role of the PA system in cancer progression is now well documented [8–12]. However, the mechanisms by which the multifunctional PA system promotes malignant progression are still not fully understood. In particular, the role of PAI-1, which has been considered for a long time as a cancer inhibitor, is still the object of a debate. The initially unexpected findings that high PAI-1 levels have a prognostic impact of

Address all correspondence to: Agnès Noel, Laboratory of Tumor and Developmental Biology, University of Liège, Tour de Pathologie (B23), Sart-Tilman, B-4000 Liège, Belgium. E-mail: agnes.noel@ulg.ac.be

[1]This work was supported by grants from the Communauté Française de Belgique (Actions de Recherches Concertées), the Commission of European Communities (FP6 no. LSHC-CT-2003-503297), the Fonds de la Recherche Scientifique Médicale, the Fonds National de la Recherche Scientifique (FNRS, Belgium), the Fédération Belge Contre le Cancer, the Fonds Spéciaux de la Recherche (University of Liège), the Centre Anticancéreux près l'Université de Liège, the FB Assurances, the Fondation Léon Frédéricq (University of Liège), the DGTRE from the "Région Wallonne," the Interuniversity Attraction Poles Program—Belgian Science Policy (Brussels, Belgium). M.J. and K.B. are recipients of a grant from FNRS-Télévie. C.M. is recipient of a grant from FRIA-FNRS.
Received 18 June 2004; Revised 30 September 2004; Accepted 2 October 2004.

DOI 10.1593/neo.04406

poor survival for patients suffering from a variety of different cancers raised questions on the functions of PAI-1 [9,13]. In this context, the surprising proangiogenic function of PAI-1 evidenced by transplanting murine tumor cells into PAI-1–deficient (PAI-$1^{-/-}$) mice has shed some lights on these paradoxic clinical data [14,15]. Furthermore, controversial data have been reported on the impact of genetic alterations in PAI-1 levels on tumor progression. One study concluded that neither PAI-1 deficiency nor PAI-1 overexpression affects tumor invasion and metastases of B16 melanoma cells [16]. Recently, lack of spontaneous phenotype in PAI-1–deficient mice was found consistent with the observation that spontaneous transgenic breast cancer was unaffected by PAI-1 deficiency [17]. In a sarcoma model, both uPA and tPA appeared more crucial for tumor growth than PAI-1 [11].

Altogether, these findings suggest that the tumor-promoting effects of PAI-1 may be dependent on the tumor type, the site of its production (tumor cells *versus* host cells), and the stage of the cancer progression. Until now, all studies investigating the impact of PAI-1 deficiency on tumor growth have been performed by transplanting murine tumor cells into syngeneic mice, or by interbreeding PAI-1–deficient mice with transgenic mice developing oncogene-driven tumors. However, up to now, no information is available regarding the putative role of PAI-1 in human skin or cervical carcinoma progression. To address this question, we have generated immunodeficient PAI-1 knockout mice in two different genetic backgrounds [nude or recombination activating gene-1 (*Rag-1*)–deficient mice]. Human malignant cervical keratinocytes and human HaCaT-*Ras* skin carcinoma cells displaying different invasive potentials have been transplanted on a collagen matrix or subcutaneously injected into these mice. In the present study, we demonstrate that PAI-1 is an essential factor of the host microenvironment, promoting early steps of skin carcinoma progression.

Materials and Methods

Genetically Modified Mice

PAI-1–deficient mice (PAI-$1^{-/-}$) and their corresponding wild type mice (WT; PAI-$1^{+/+}$) with a mixed genetic background of 87% C57BL/6 and 13% 129 strain were mated with Rag-1–deficient mice (Rag-$1^{-/-}$: B6; 129S-Rag-$1^{tm/Mom}$/J) purchased from Charles Rivers Laboratories (L'Arbresle, France). F1 offspring were heterozygous for both genes. The F2 offspring of the F1 interbreeding were screened by FACS analysis for the absence of CD4, CD8, and CD3 (Becton Dickinson, San Diego, CA) or the presence of thy 1.2 expression (as positive control) (Becton Dickinson) on whole blood lymphocytes (data not shown). The resulting mice identified as Rag-$1^{-/-}$ were screened for PAI-1–null allele. DNA was extracted from tail biopsies (genomic DNA extraction kit from tissue; Macherey-Nagel, Düren, Germany), amplified by polymerase chain reaction (PCR) with *Taq* DNA polymerase (Takara) and a PCR mix including three primers to discriminate between WT, heterozygous, and homozygous mice: PAI-2312 (5′-GACCTTGC CAAGGTGATGCTTGGCAAC-3′) and PAI-2726 (5′-GAGTGGCCTGCTAGGAAATTCA TTC-3′) annealing in the PAI-1 gene (accession no. M33960), and PGKPA (5′-AA TGTGTCAGTTTCATAGCC-3′) annealing in the knockout construct. The PCR conditions included an initial denaturation step at 95°C for 5 minutes, followed by 35 cycles at 94°C for 1 minute, 60°C for 1 minute, 72°C for 1 minute, and a final extension step at 72°C for 5 minutes. The reaction products were analysed by electrophoresis on 2% agarose gel. The size of the amplified fragment was 400 bp for WT mice, 190 and 400 bp for PAI-$1^{+/-}$ mice, and 190 bp for PAI-$1^{-/-}$ mice. All animals used were 2 months old and were maintained under specific pathogen-free conditions, with 12-hour light/12-hour dark cycle and had free access to food and water.

Nude mice were generated by backcrossing C57B16J/129 PAI-1 heterozygous mice into the META/Bom substrain of BALB/c for five passages. Littermate offspring were made by mating a PAI-$1^{+/-}$ META/Bom nu/nu male with a PAI-$1^{+/-}$ female of the META/Bom nu/+ genotype. In all experiments involving wild-type mice as controls, these were littermates to the PAI-1 gene–deficient mice.

Cell Lines and Culture

The malignant HaCaT II-4 clone was derived from human HaCaT keratinocytes after transfection with the mutated val-12-Harvey-*Ras* oncogene (HaCaT-*Ras* cells) [18]. HaCaT A5-RT3 clone was established by recultivation *in vitro* of subcutaneous tumors derived from HaCaT-*Ras* cells and retransplanted three times *in vivo*. These two cell lines with HaCaT II-4 (forming well differentiated SCCs) and HaCaT A5-RT3 (growing to poorly differentiated SCCs with local lymph node metastases) display different tumorigenic potentials [19]. The Caski cell line is an HPV16-transformed cervical cell line [20].

Malignant HaCaT cells were cultivated in modified Eagle's medium containing a four-fold concentration of essential amino acids and vitamins (GIBCO BRL, Paisley, UK), 10% fetal bovine serum (FBS) (GIBCO BRL), penicillin (100 U/ml), and streptomycin (100 μg/ml). The growth medium used for CasKi cells was a 1:3 mixture of Ham's F12/Dulbecco's modified Eagle's medium (GIBCO BRL), supplemented with 0.4 μg/ml hydrocortisone (Sigma Chemical Co., St Louis, MO), 2 ng/ml epidermal growth factor (Sigma), 10% FBS (GIBCO BRL), 2 mM L-glutamine (GIBCO BRL), 1 mM sodium pyruvate (GIBCO BRL), penicillin (100 U/ml), streptomycin (100 μg/ml) (GIBCO BRL), 5 μg/ml insulin (Sigma), 20 μg/ml adenine (Sigma), 5 μg/ml human transferrin (Sigma), and 15×10^{-4} μg/ml 3,3′,5-triiodo-L-thyronine (Sigma). Cells were maintained in a humidified incubator at 37°C with 5% CO_2.

For transplantation assay, cells (2×10^5) were plated on a collagen gel (4 mg/ml type I collagen isolated from rat tail tendons) inserted in Teflon rings (Renner GmbH, Darmstadt, Germany) and maintained in culture for 1 day before grafting in mice.

Reverse Transcriptase PCR Analysis

Total RNA from HaCaT II-4 and HaCaT A5-RT3 cells was extracted using the High Pure RNA isolation kit (Roche Diagnostics, Mannheim, Germany). RT-PCR amplification was performed using the GeneAmp Thermostable rTth reverse transcriptase RNA PCR kit (Perkin Elmer Life Sciences, Boston, MA), specific pairs of primers (5 pmol each) (Table 1), and 10 ng of total RNA per 25 μl of reaction mixture (final volume). Reverse transcription was performed at 70°C for 15 minutes. For uPA and PAI-1 transcripts, PCR amplification was run as follows: 15 seconds at 94°C, 20 seconds at 68°C, 10 seconds at 72°C (number of cycles as indicated in Table 1), followed by a final 2-minute extension step at 72°C. Other cycling conditions are the followings: 20 seconds at 94°C, 30 seconds at 64°C, 20 seconds at 72°C for tPA, α_V and β_3 integrin; and 20 seconds at 94°C, 30 seconds at 60°C, and 20 seconds at 72°C for uPAR and 28S. RT-PCR products were resolved on 10% polyacrylamide gels and analysed using a Fluor-S MultiImager (Bio-Rad, Hercules, CA) after staining with Gelstar dye (FMC BioProducts, Heidelberg, Germany). The selected primer pairs are described in Table 1.

Enzymatic Assay

HaCaT II-4 and HaCaT A5-RT3 cells were plated at 10^5 cells/well in a 12-well culture plate. After 2 days of culture, cells were rinsed twice with PBS and left in serum-free medium with or without Plg (5 μg/ml; Roche Diagnostics), amiloride, a specific uPA inhibitor (200 μg/ml; Sigma), or α_2-antiplasmin (3 μg/ml; Sigma). After 24 hours of incubation time, the conditioned media were harvested, centrifuged for 5 minutes at 5×10^3 *g*, and then concentrated 10-fold by centrifugation (Amicon Ultra-4 10^4 MW; Millipore, Bedford, MA). Fifty microliters of 10-fold concentrated conditioned media was incubated in 50 mM Tris/HCl, pH 7.4, 100 mM NaCl, 0.01% Tween-20, and 100 μM H-Ala-Phe-Lys-AMC (Bachem, Weil am Rhein, Germany), a fluorogenic plasmin substrate, for 200 seconds at 37°C. Fluorescence was measured in a Microplate Fluorometer (SpectraMax GeminiXS; Molecular Devices, Bedford, MA) at 380 nm (excitation) and 460 nm (emission). Results are expressed as fluorescent arbitrary unit normalized to cell DNA content.

Transplantation Assay in Mice

The cell-coated collagen gels were covered with a silicone transplantation chamber (Renner GmbH) and implanted *in toto* onto the dorsal muscle fascia of mice as described previously [14,21]. Three weeks later, transplants were resected, embedded in Tissue Tek (Miles Laboratories, Inc., Naperville, IL), and frozen in liquid nitrogen for cryostat sectioning.

In all assays, the take rate and growth of transplants were verified by classic histology, and some samples were not taken into account. The exclusion criteria were the loss of transplantation chamber, the absence of cells on top of the collagen gel, and the failure of collagen gel adherence onto the host tissue with the consequence of poor cell growth. Based on the two latter parameters, 11% of samples resected from WT mice and 35% of samples resected from PAI-$1^{-/-}$ mice were excluded (in both immunodeficient backgrounds). These differences reflect the lower remodeling and infiltration of the collagen gel by host cells in PAI-$1^{-/-}$ mice. Chambers were lost in 7% of WT mice and 11% of PAI-$1^{-/-}$ mice.

Subcutaneous Injection

Cells were inoculated subcutaneously (2×10^6 cells in 200 μl of culture medium per site) into each flank of the animals. Tumor incidence was defined as the percentage of mice presenting a tumor having a volume of at least 50 mm^3.

Table 1. Sequence of Primers Used for RT-PCR Studies.

Gene (Accession No.)	Position	Oligonucleotide Sequence (5′–3′)	Cycles (*n*)
28S (U13369)	12403F	GTTCACCCACTAATAGGGAACGTGA	17
	12614R	GATTCTGACTTAGAGGCGTTCAGT	
PAI-1 (M16006)	464F	AGGGCTTCATGCCCCACTTCTTCA	30
	655R	AGTAGAGGGCATTCACCAGCACCA	
uPA (NM_002658)	1122F	ACTACTACGGCTCTGAAGTCACCA	30
	1321R	GAAGTGTGAGACTCTCGTGTAGAC	
tPA (NM_033011)	362F	CAGCAGGCCCTGTACTTCTC	37
	633R	GGCTTTGAGTCTCGATCTGG	
uPAR (U08839)	901F	CTGGAGCTTGAAAATCTGCCG	30
	1057R	GGTTTTTCGGTTCGTGAGTGC	
α_V (NM_002210)	2328F	CGAAACAATGAAGCCTTAGCAAGA	30
	2605R	GGACTCGAGACTCCTCTTATCTCA	
β_3 (NM_000212)	782F	GGCTACAGTCTGTGATGAAAAGAT	35
	1153R	CGGATTTTCCCATAAGCATCAACA	

Immunofluorescence Staining

Cryostat sections (6 μm thick) were fixed in acetone at −20°C and 80% methanol at 4°C for 10 minutes, permeabilised in 1% Triton X-100 for 10 minutes, and then incubated with the primary antibodies (Abs). Abs against fibrinogen (goat antimouse) and against VEGF (rabbit antihuman) were purchased from Nordic Immunology (Tilburg, The Netherlands) and Santa Cruz Biotechnology (Santa Cruz, CA), respectively. For double immunofluorescence labeling studies, sections were first incubated for 2 hours at 37°C with the two primary Abs: anti–type IV collagen Ab (guinea pig polyclonal Ab) [22] and anticytokeratin Ab (rabbit polyclonal Ab, diluted 1/200, catalog no. Z0622; Dako, Glostrup, Denmark). The sections were washed in PBS (3 × 10 minutes) before the incubation with appropriate secondary Abs conjugated to fluorescein–isothiocyanate (FITC) or tetramethyl-rhodamine isothiocyanate (TRITC): goat anti–guinea pig IgG (diluted 1/100; ICN Costa Mesa, CA) and monoclonal antirabbit Abs (diluted 1/40; Dako) were applied for 30 minutes at room temperature. The sections were washed three times in PBS for 10 minutes each and coverslips were mounted with Aqua Polymount (Polysciences, Warrington, FL). The specific labeling was observed using an inverted microscope equipped with epifluorescence optics.

The assessment of apoptotic cell death was performed by detecting DNA strand breaks by the terminal deoxynucleotidyl transferase (TdT)–mediated dUTP nick-end labeling (TUNEL) method. Cryostat sections fixed in 4% paraformaldehyde for 20 minutes and in methanol for 5 minutes were stained for apoptosis following the manufacturer's instructions (Roche Diagnostics).

Morphometric Analysis of Angiogenesis and Tumor Cell Invasion

Morphometric assessment of angiogenesis was scored as previously described [23]. A score of (−) means that vessels were undetected in the collagen gel. When blood vessels infiltrate the collagen gel and get into close contact with the malignant epithelial layer, a score of (++) is assigned. A score of (+++) indicates that vessels infiltrated the tumor parenchyma so that invasive epithelial tumor sprouts and vessels are intermingled. Morphometric measurements of tumor cell invasion (average distance of invasion) were performed by using a computer-assisted image analysis system (Quantimet 600 imaging; Leica, Van Hopplynus, Brussels, Belgium). The depth of tumor invasion was determined by measuring the distance between the top of the tumor cell layer and the deepest tumor sprouts [24]. An average distance of invasion was calculated from at least 10 measurements per tumor section.

Statistical Analysis

DATA were analyzed on a computer (GraphPad Prism). The chi-square analysis was used to determine whether there were significant differences in angiogenesis scores between control and genetically modified mice. Quantification results of tumor invasion were statistically analysed using two-tailed Student's *t* test. Tumor incidence data were analysed with the log rank test. For all experimental conditions, $P < .05$ was considered as significant.

Results

Tumor Cell Transplantation Into PAI-1$^{-/-}$ and WT Nude Mice

The invasive and angiogenic phenotypes of two malignant human cutaneous keratinocytes (HaCaT II-4 and HaCaT A5-RT3) were compared in the surface transplantation assay. We first compared the production of various components of the Plg/plasmin cascade in these two cell lines. An RT-PCR analysis revealed that these cells expressed the different components of the PA system (uPA, uPAR, and PAI-1) at similar levels (Figure 1). Low levels of tPA mRNA were detected in both cell lines (Figure 1). To determine PA activities, hydrolysis of plasmin fluorogenic substrate was quantified in the medium conditioned by cells. Addition of exogenous Plg led to a strong hydrolysis of the plasmin substrate, which was completely inhibited by α_2-antiplasmin. The plasmin activity observed on Plg addition was similar in medium conditioned by HaCaT II-4 (fluorescent arbitrary unit/μg DNA = 416.8 ± 36.1) and HaCaT A5-RT3 (fluorescent arbitrary unit/μg DNA = 357 ± 56.7) ($P > .05$). A 70% reduction of plasmin activity was observed in both conditioned media after addition of amiloride, an uPA inhibitor (fluorescent arbitrary unit/μg DNA = 124.4 ± 20.7 and 113.9 ± 21.7 for HaCaT II-4 and HaCaT A5-RT3, respectively) ($P < .01$). This demonstrates that Plg-to-plasmin conversion is mainly mediated by uPA in both cell types. Similar amounts of PAI-1 were produced by both cell lines as assessed by ELISA (3.2 and 3.4 ng/ml for HaCaT II-4 and HaCaT A5-RT3, respectively). Because

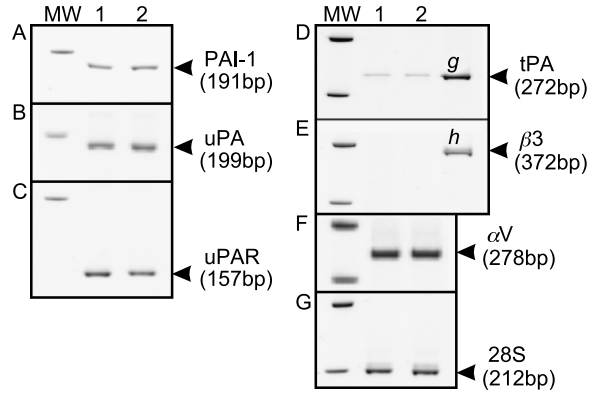

Figure 1. *Expression of components of the Plg/plasmin cascade and of integrins by HaCaT clones. Total RNA were extracted from HaCaT A5-RT3 (1) and HaCaT II-4 (2). RT-PCR analyses were performed for PAI-1 (A), uPA (B), uPAR (C), tPA (D), β_3 subunit (E), and α_V subunit (F) of integrins. In some assays, RNA isolated from glioblastomas (D) or human umbilical vein cells (HUVECs) (E) have been added as positive controls. 28S ribosomal RNA is shown as a loading control (G). The expected sizes of amplified mRNAs are indicated on the right. g = glioblastomas; h = HUVEC.*

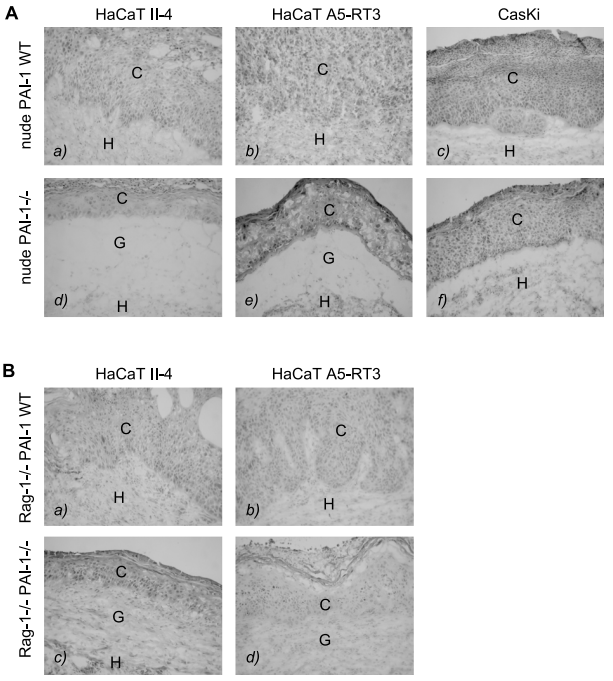

Figure 2. *In vivo growth and invasive behavior of malignant human keratinocytes. (A) HaCaT II-4 (a and d), HaCaT A5-RT3 (b and e), and CasKi (c and f) cells were transplanted for 3 weeks into WT (a–c) and PAI-1$^{-/-}$ (d–f) nude mice. (B) HaCaT II-4 (a and c) and HaCaT A5-RT3 (b and d) cells were transplanted for 3 weeks into WT (a and b) and PAI-1$^{-/-}$ (c and d) Rag-1$^{-/-}$ mice. Histological sections were stained with hematoxylin and eosin. C = carcinoma cells; G = collagen gel; H = host connective tissue. Original magnification, × 200.*

PAI-1 function may be related to its capacity to interact with $\alpha_V\beta_3$ integrin, the expression of these two integrin subunits was analyzed by RT-PCR (Figure 1). Although both cell lines produced the α_V subunit at similar extent, they did not express the β_3 subunit (Figure 1).

After this expression profiling analysis, cells cultured on a collagen gel were implanted onto the dorsal muscle fascia of WT and PAI-1$^{-/-}$ nude mice. Such a grafting in WT mice led to a remodeling of the collagen matrix, infiltration by host-derived cells, and a progressive replacement by a highly vascularized granulation tissue [14,25]. Three weeks after grafting into WT mice, both cell types formed a multilayered, poorly organized epithelium infiltrated by stromal strands containing capillaries (Figure 2*A*). In sharp contrast, when HaCaT A5-RT3 or HaCaT II-4 cells were implanted into PAI-1–deficient mice, a significant reduction in host connective tissue formation and in tumor growth and invasion was observed. As a consequence, most of the collagen matrix persisted below the stratified epithelial layers (Figure 2*A*).

Cancer invasion was determined by measuring the maximal depth of penetration of individual tumor sprouts and by calculating the average distance of invasion. Both HaCaT II-4 and A5-RT3 penetrated more deeply into WT host tissue (231.7 ± 15.97 μm and 585.4 ± 109.8 μm , respectively) than into PAI-1–deficient tissue (103.2 ± 7.72 μm and 210.6 ± 53.82 μm, respectively) ($P < .02$) (Figure 3, *a* and *b*).

Tumor angiogenesis was visualized after staining for collagen type IV to delineate capillary basement membrane

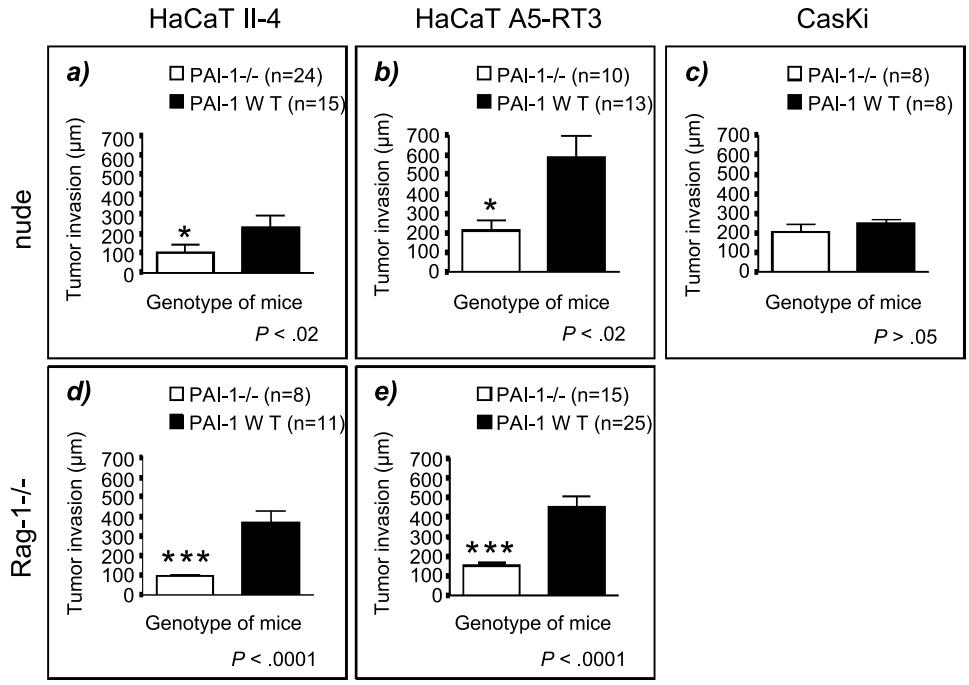

Figure 3. *Morphometric assessment of tumor cell invasion implanted into nude or Rag-1$^{-/-}$ mice. HaCaT II-4 (a and d), HaCaT A5-RT3 (b and e), and CasKi (c) tumor cells were grafted for 3 weeks into PAI-1$^{-/-}$ (white bars) and control (black bars) mice in nude (a–c) or Rag-1$^{-/-}$ (d and e) background. Tumor cell invasion was estimated by measuring the distance between the top of the tumor to the deepest front of tumor spread. n = number of animals per group. *P ≤ .02, ***P ≤ .0001, Student's t test. Data are expressed as mean ± standard error of the mean.*

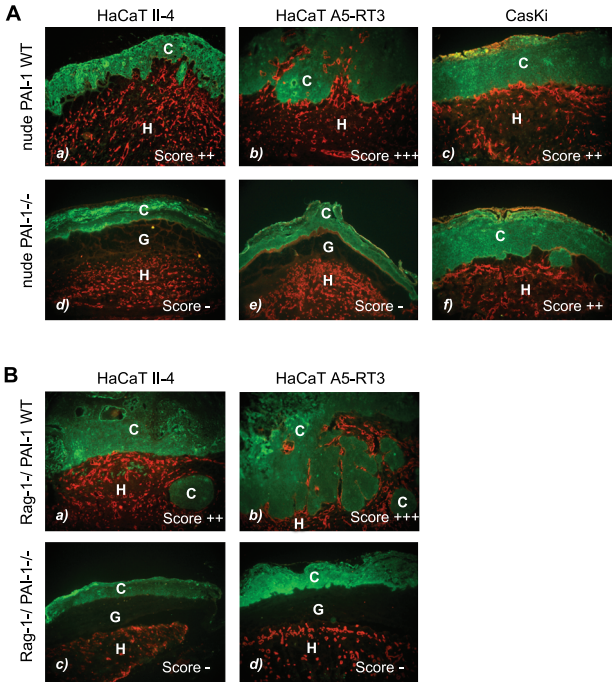

Figure 4. *Immunofluorescence labeling of malignant keratinocytes and vessels in transplants grafted in nude (A) or Rag-1$^{-/-}$ (B) mice. (A) HaCaT II-4 (a and d), HaCaT A5-RT3 (b and e), and Caski (c and f) cells were implanted for 3 weeks into WT (a–c) and PAI-1$^{-/-}$ (d–f) nude mice. (B) HaCaT II-4 (a and c) and HaCaT A5-RT3 (b and d) cells were grafted for 3 weeks into WT (a and b) and PAI-1$^{-/-}$ (c and d) Rag-1$^{-/-}$ mice. Malignant cells were detected on cryostat sections by using anticytokeratin Ab (green), and vessels were detected using an anticollagen type IV Ab (red). At all times after grafting, collagen type IV labelings were codistributed with endothelial cells recognized by antimouse platelet endothelial cell adhesion molecule (PECAM) immunostaining (data not shown). C = carcinoma cells; G = collagen gel; H = host connective tissue. Original magnification, × 100.*

(Figure 4*A*) or for CD31/PECAM (data not shown) and semiquantitatively scored (Figure 5). Whereas vessels had reached the epithelial–stromal border and had penetrated the tumor parenchyma in wild-type animals, they stayed apart in PAI-1–deficient mice separated from the epithelium by the remnant collagen matrix. In accordance with their more aggressive phenotype, about 70% of WT mice grafted with HaCaT A5-RT3 cells were scored as (+++) (Figure 5*b*), whereas all HaCaT II-4 tumors were scored as (++) in WT mice (Figure 5*a*). After transplantation into PAI-1$^{-/-}$ nude mice, a reduction of tumor vascularization was detected for both cell types. In the absence of host PAI-1, none of the HaCaT A5-RT3 tumors was scored (+++) and 50% of samples were scored (–) and (++) ($P < .01$) (Figure 5*b*). Most of the HaCaT II-4 tumors (63%) were scored (–) ($P < .01$) (Figure 5*a*). Therefore, PAI-1$^{-/-}$ mice exhibited significantly reduced tumor invasion and vascularization for both squamous carcinoma cells in comparison to WT mice.

To determine whether the tumor-promoting effect of PAI-1 is specific to the type of tumor cell used, the behavior of malignant human cervical keratinocytes (Caski cells) was investigated (Figures 2*A* and 4*A*). Tumor tissues were developed, exhibiting about the same thickness (204.9 ± 37.41 μm in PAI-1$^{-/-}$ *vs* 246.7 ± 20.05 μm in WT mice; $P > .05$) although without pronounced invasion and were vascularized to a similar degree (score ++) in both genotypes (Figures 3*c* and 5*c*). Vascularization, however, was more pronounced at the tumor border in WT than in PAI-1–deficient animals.

Tumor Cell Transplantation Into PAI-1$^{-/-}$ and WT Rag-1$^{-/-}$ Mice

We next investigated the angiogenic and invasive phenotypes of HaCaT A5-RT3 and HaCaT II-4 cells in another PAI-1$^{-/-}$ and WT background, the Rag-1$^{-/-}$ mice. In WT mice, the histologic aspect of the HaCaT II-4 and HaCaT A5-RT3 tumors was similar to that observed in nude mice. Lack of host PAI-1 resulted in a significant reduction of tumor development (Figures 2*B* and 3, *d* and *e*) and vascularization (Figures 4*B* and 5, *d* and *e*) for both tumor types. Again, the distance of tumor invasion as well as the tumor mass were higher in WT mice than in PAI-1$^{-/-}$ mice (368.3 ± 56.68 μm *vs* 95.52 ± 7.37 μm for HaCaT II-4 cells, and 451.5 ± 54.41 μm *vs* 150.9 ± 16.58 μm for HaCaT A5-RT3 cells) ($P < .0001$) (Figure 3, *d* and *e*). Similarly, the scoring of tumor vascularization revealed a reduced angiogenic response in the absence of host PAI-1 (Figure 5, *d* and *e*).

Immunohistochemical Analysis of Tumor Transplants

We carried out an immunohistochemical analysis of tumors transplanted into PAI-1–proficient or –deficient mice, in both genetic backgrounds (nude or Rag-1$^{-/-}$). We first investigated the deposition of fibrin as an end-point of a plasmin-mediated fibrinolysis and as a provisional matrix for cell migration and invasion. Lack of host PAI-1 did not lead to any obvious modification of fibrin(ogen) deposition, suggesting that fibrinolysis was not changed in the absence of PAI-1 (data not shown). Although a decrease of VEGF production has been reported in the absence of PAI-1 [15,26], no difference of VEGF staining was evidenced in our transplantation system (data not shown). Similarly, TUNEL stainings for apoptotic cells indicated that the extent of apoptosis was always low in the cancer cell layers, in endothelial cells of blood vessels associated to the stromal strands of WT tumors, or in blood vessels remaining below the collagen gel in PAI-1$^{-/-}$ mice (data not shown).

Subcutaneous Growth of Cells Injected Into WT or PAI-1$^{-/-}$ Mice

The *in vivo* tumorigenicity of the two HaCaT variants was next evaluated by subcutaneous inoculation into PAI-1$^{-/-}$ mice and their control counterpart, in both nude and Rag-1$^{-/-}$ backgrounds. As shown in Figure 6, the tumor incidence in nude PAI-1$^{-/-}$ mice injected with HaCaT II-4 was significantly decreased as compared to that observed in WT mice ($P < .05$). Indeed, 38 days after cell injection, HaCaT II-4 cells gave rise to 100% tumors in WT mice and 62.5% in PAI-1–deficient mice (Figure 6*A*). A reduction of tumor incidence was also observed in the Rag 1$^{-/-}$ background (Figure 6*B*). In sharp contrast, within 2 or 3 weeks, the more aggressive HaCaT A5-RT3 cells gave

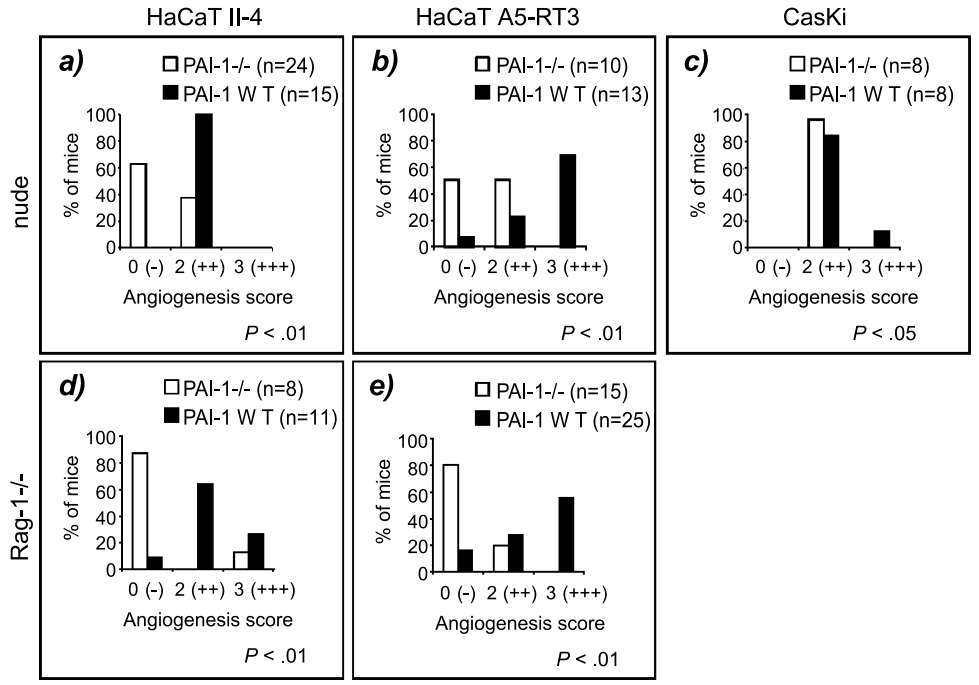

Figure 5. *Semiquantitative analysis of angiogenesis of tumors transplanted into nude or Rag-1$^{-/-}$ mice. HaCaT II-4 (a and d), HaCaT A5-RT3 (b and e), and CasKi (c) tumor cells were grafted for 3 weeks into PAI-1$^{-/-}$ (white bars) and WT (black bars) mice in a nude (a–c) or Rag-1$^{-/-}$ (d and e) background. Morphometric assessment of angiogenesis was scored as follows: vessels undetected in the collagen gel: score (–); blood vessels infiltrating the collagen gel and getting in close apposition to the epithelial layer: score (++); and blood vessels intermingling with invasive epithelial tumor sprouts: score (+++). n = number of animals per group. Chi-square analysis was used; P is indicated.*

rise to 80% to 100% of tumors in mice regardless of PAI-1 status and in both nude and Rag-1 backgrounds (Figure 6).

To better define the process leading to a reduction of HaCaT II-4 tumor incidence in PAI-1$^{-/-}$ mice, tumor growth was also evaluated. We observed that once the tumors were established, the increase of tumor volumes was identical in both genotypes and was not dependent on the expression levels of host PAI-1 (data not shown). These data suggest that PAI-1 displays a growth-promoting effect for poorly aggressive cancer cells during early stages of tumor growth, but is dispensable when the tumor is undergoing expansion. In the case of more aggressive tumors (HaCaT

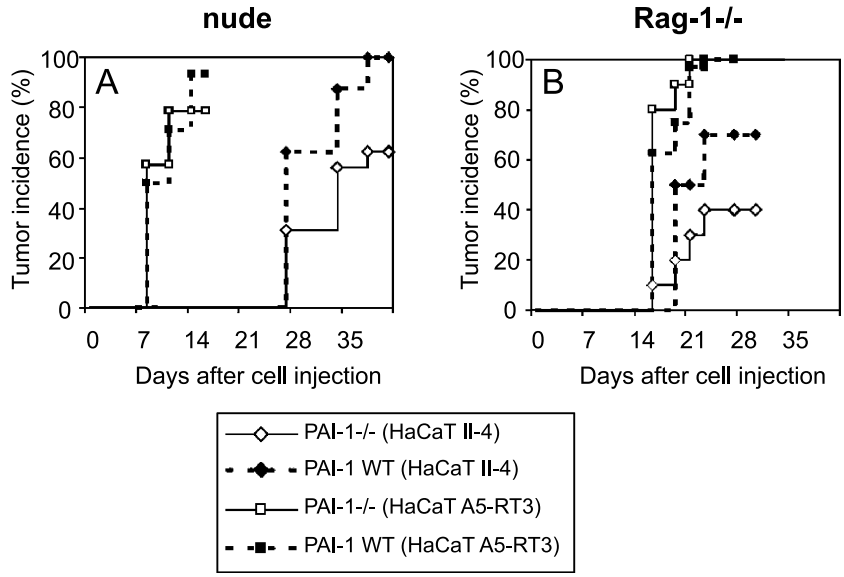

Figure 6. *Analysis of HaCaT II-4 and HaCaT A5-RT3 malignant cutaneous cell tumorigenicity in PAI-1$^{-/-}$ and WT nude (A) and Rag-1$^{-/-}$ (B) mice. The incidence corresponds to the percentage of animals bearing palpable tumors (volume >50 mm^3). Each experimental group includes 10 mice.*

A5-RT3 cells), consistent with the effect on tumor incidence (Figure 6), the growth rate was similar in the absence or presence of host PAI-1 (data not shown).

Discussion

The onset of invasion represents an early step in the conversion of a carcinoma *in situ* to a malignant squamous cell carcinoma (SCC) with the capacity to spread and to eventually metastasize. Angiogenesis and tumor vascularization appear as a crucial prerequisite for invasion [21,27]. Angiogenesis involves a tightly controlled orchestration of complex interactions between tumor cells, host cells, soluble factors, and ECM components that lead to the formation of new blood vessels. The specific functions of the *in vivo* microenvironment in controlling the invasive and angiogenic phenotypes of tumor cells are still poorly understood. However, the recent generation of targeted gene–deficient mice has been helpful to identify individual genes playing a key role during tumor growth and vascularization. In this context, PAI-1 hasbeen identified as a crucial element of the Plg/PA system controlling *in vivo* tumor angiogenesis [14,15,23]. Although much has been learned on murine tumor development utilizing PAI-$1^{-/-}$ mice, no experimental data are available regarding the role of PAI-1 in human cancer progression. In the present study, immunodeficient PAI-$1^{-/-}$ mice have been generated in two different genetic backgrounds (Rag-$1^{-/-}$ or nude nu/nu). Two separate sets of experiments including 8 to 24 mice per genotype (PAI-$1^{-/-}$ and their corresponding WT) in both immunodeficient genetic backgrounds demonstrated the dramatic effect of host PAI-1 absence on SCC growth and vascularization. The present study provides evidence that PAI-1 in these models is a crucial determinant of tumor microenvironment in regulating and enhancing early stages of human skin carcinoma invasion.

When two different human cell lines were transplanted as a precultured epithelium on a collagen gel (surface transplantation system), both tumor invasion and vascularization were reduced in PAI-1–deficient mice. In accordance with their more aggressive phenotype, HaCaT A5-RT3 transplants were much more vascularized (score +++) in WT mice than HaCaT II-4 transplants. A significant reduction of the invasive and angiogenic phenotypes of both HaCaT II-4 and HaCaT A5-RT-3 cells was determined by objective morphometric quantification. This important effect of PAI-1 deficiency on tumor progression emphasizes the key role played by host cells during this process. With low tumor cell numbers, PAI-1 produced by neoplastic cells is not sufficient to circumvent host deficiency. Indeed, by transfecting malignant keratinocytes with PAI-1 cDNA, we previously showed that PAI-1 produced by tumor cells, even at high concentration, did not overcome the absence of PAI-1 in the host tissue [24]. The present data provide the first experimental evidence for a role of stromal PAI-1 in human skin cancer invasion and vascularization.

Although the precise mechanism of PAI-1 action is not well understood, several lines of evidence indicate that PAI-1 effects result from a tight control of extracellular proteolysis and/or a regulation of cell detachment and migration by its interaction with vitronectin and integrins [28,29]. By using adenoviral delivery of mutated forms of PAI-1, we have previously demonstrated that PAI-1 facilitates tumor angiogenesis [23,30] or laser-induced choroidal angiogenesis [31] by inhibiting proteolytic activity rather than by interacting with vitronectin. In the present study, the lack of β_3 integrin subunit expression by the cells used is consistent with a PAI-1–mediated regulation of angiogenesis without involvement of integrins. The requirement of a good balance between PA and PAI-1 is supported by recent data showing that the proangiogenic and antiangiogenic effects of PAI-1 are dose-dependent [24,30,32,33]. In other models, PAI-1 effects have been ascribed to both antiprotease and vitronectin-binding functions [28,34]. Because PAI-1 is a multifunctional molecule, it is likely that its mechanisms of action are dependent on the tumor types and/or on the stage of cancer progression. Host PAI-1 did not affect the extent of apoptosis of tumor cells and/or stromal cells as assessed by TUNEL stainings (data not shown). This is consistent with a previous report of recombinant PAI-1 administration into mice bearing melanomas [33]. *In vivo* studies have reported a decrease in VEGF expression in the absence of PAI-1 [15,26]. However, by immunohistochemical analysis, similar VEGF stainings were detected in tumor cell transplants in the absence or presence of PAI-1. We cannot exclude the possibility that VEGF produced by tumor cells can compensate for a putative regulation of stromal VEGF expression in the absence of PAI-1. However, our data are in accordance with the identical levels of both VEGF transcripts and proteins evidenced in aortic endothelial cells isolated from WT and PAI-$1^{-/-}$ mice [35]. It has been proposed that alterations in the rate of cell proliferation in PAI-$1^{-/-}$ endothelial cells may affect vessel formation and stability [35]. However, by using the surface transplantation system, similar numbers of vessels were detected below the collagen gels in both WT and PAI-$1^{-/-}$ mice, thus reflecting an identical angiogenic response induced below the transplant in both genotypes [14]. This suggests that inhibition of angiogenesis is more related to impaired ability of endothelial cells to infiltrate an ECM or the tumor parenchyma rather than to an aberrant proliferation rate. This is consistent with the defective spreading of endothelial cells from aortic fragments issued from PAI-$1^{-/-}$ mice [30]. The impaired angiogenesis was not related to the use of a collagen type I matrix because tumor cell implantation in the presence of Matrigel led to similar dependency on host PAI-1 [24].

Cells were also subcutaneously inoculated into WT or PAI-$1^{-/-}$ mice. The lack of PAI-1 significantly reduced the incidence of subcutaneous tumors derived from poorly aggressive HaCaT II-4 cells, but not the incidence of tumors derived from the more aggressive HaCaT A5-RT3 cells. However, in both cases, once implanted, the proliferation rate of tumors was not dependent on the PAI-1 status of host tissue. These data emphasize the importance of PAI-1 in the early steps of cancer progression and confirmed our recent study using murine PDVA cells [24]. A similar observation

was already done for stromelysin-3 (MMP-11), which appears to control tumor cell apoptosis [36–38]. Such a specific effect of PAI-1 in early events of cancer progression rather than during the course of cancer expansion may provide an explanation for some of the apparently contradictory reports in the literature. Also, the number of transplanted/injected tumor cells and their production of tumor cell–derived PAI-1 may account for the differences seen in surface transplants (low cell number) and subcutaneous tumors (10 times higher injected cell number) concerning the effects on tumor growth and invasion. In addition, the absence of PAI-1 effect on the evolution of tumors induced by human cervical CasKi cell transplantation suggests that PAI-1 is not a universal proangiogenic factor and that its effect may be tumor type–dependent or tumor stage–dependent [6].

In conclusion, our data provide new insights into the function of an individual component of the Plg/PA system, host PAI-1, in specific steps of human cancer implantation. Interestingly, it extends the importance of PAI-1 to human skin carcinomas.

Acknowledgements

We thank I. Dasoul, P. Gavitelli, F. Olivier, and M. R. Pignon for their excellent technical assistance.

References

[1] Dano K, Romer J, Nielsen BS, Bjorn S, Pyke C, Rygaard J, and Lund LR (1999). Cancer invasion and tissue remodeling—cooperation of protease systems and cell types. *APMIS* **107,** 120–127.

[2] Noel A, Albert V, Bajou K, Bisson C, Devy L, Frankenne F, Maquoi E, Masson V, Sounni NE, and Foidart JM (2001). New functions of stromal proteases and their inhibitors in tumor progression. *Surg Oncol Clin N Am* **10,** 417–432.

[3] Naldini L, Tamagnone L, Vigna E, Sachs M, Hartmann G, Birchmeier W, Daikuhara Y, Tsubouchi H, Blasi F, and Comoglio PM (1992). Extracellular proteolytic cleavage by urokinase is required for activation of hepatocyte growth factor/scatter factor. *EMBO J* **11,** 4825–4833.

[4] Vakili J, Standker L, Detheux M, Vassart G, Forssmann WG, and Parmentier M (2001). Urokinase plasminogen activator and plasmin efficiently convert hemofiltrate CC chemokine 1 into its active. *J Immunol* **167,** 3406–3413.

[5] Hertig A, Berrou J, Allory Y, Breton L, Commo F, Costa De Beauregard MA, Carmeliet P, and Rondeau E (2003). Type 1 plasminogen activator inhibitor deficiency aggravates the course of experimental glomerulonephritis through overactivation of transforming growth factor beta. *FASEB J* **17,** 1904–1906.

[6] Noel A, Maillard C, Rocks N, Jost M, Chabottaux V, Sounni NE, Maquoi E, Cataldo D, and Foidart JM (2004). Membrane associated proteases and their inhibitors in tumour angiogenesis. *J Clin Pathol* **57,** 577–584.

[7] Rakic JM, Maillard C, Jost M, Bajou K, Masson V, Devy L, Lambert V, Foidart JM, and Noel A (2003). Role of plasminogen activator–plasmin system in tumor angiogenesis. *Cell Mol Life Sci* **60,** 463–473.

[8] Look MP, van Putten WL, Duffy MJ, Harbeck N, Christensen IJ, Thomssen R, Kates R, Spyratos F, Ferno M, Eppenberger-Castori S, et al. (2002). Pooled analysis of prognostic impact of urokinase-type plasminogen activator and its inhibitor PAI-1 in 8377 breast cancer patients. *J Natl Cancer Inst* **94,** 116–128.

[9] Schmitt M, Wilhelm OG, Reuning U, Krüger A, Harbeck N, Lengyel E, Graeff H, Gänsbacher B, Kessler H, Bürgle M, et al. (2000). The urokinase plasminogen activator system as a novel target for tumor therapy. *Fibrinolysis Proteolysis* **14,** 114–132.

[10] Andreasen PA, Egelund R, and Petersen HH (2000). The plasminogen activation system in tumor growth, invasion, and metastasis. *Cell Mol Life Sci* **57,** 25–40.

[11] Curino A, Mitola DJ, Aaronson H, McMahon GA, Raja K, Keegan AD, Lawrence DA, and Bugge TH (2002). Plasminogen promotes sarcoma growth and suppresses the accumulation of tumor-infiltrating macrophages. *Oncogene* **21,** 8830–8842.

[12] Duffy MJ (2004). The urokinase plasminogen activator system: role in malignancy. *Curr Pharm Des* **10,** 39–49.

[13] Pedersen H, Brunner N, Francis D, Osterlind K, Ronne E, Hansen K, Dano K, and Grondahl-Hansen J (1994). Prognostic impact of urokinase, urokinase receptor, and type 1 plasminogen activator inhibitor in squamous and large cell lung cancer tissue. *Cancer Res* **54,** 4671–4675.

[14] Bajou K, Noel A, Gerard RD, Masson V, Brunner N, Holst-Hansen C, Skobe M, Fusenig NE, Carmeliet P, Collen D, and Foidart JM (1998). Absence of host plasminogen activator inhibitor 1 prevents cancer invasion and vascularization. *Nat Med* **4,** 923–928.

[15] Gutierrez LS, Schulman A, Brito-Robinson T, Noria F, Ploplis VA, and Castellino FJ (2000). Tumor development is retarded in mice lacking the gene for urokinase-type plasminogen activator or its inhibitor, plasminogen activator inhibitor-1. *Cancer Res* **60,** 5839–5847.

[16] Eitzman DT, Krauss JC, Shen T, Cui J, and Ginsburg D (1996). Lack of plasminogen activator inhibitor-1 effect in a transgenic mouse model of metastatic melanoma. *Blood* **87,** 4718–4722.

[17] Almholt K, Nielsen BS, Frandsen TL, Brunner N, Dano K, and Johnsen M (2003). Metastasis of transgenic breast cancer in plasminogen activator inhibitor-1 gene-deficient mice. *Oncogene* **22,** 4389–4397.

[18] Boukamp P, Stanbridge EJ, Foo DY, Cerutti PA, and Fusenig NE (1990). *c-Ha-ras* oncogene expression in immortalized human keratinocytes (HaCaT) alters growth potential *in vivo* but lacks correlation with malignancy. *Cancer Res* **50,** 2840–2847.

[19] Mueller MM, Peter W, Mappes M, Huelsen A, Steinbauer H, Boukamp P, Vaccariello M, Garlick J, and Fusenig NE (2001). Tumor progression of skin carcinoma cells *in vivo* promoted by clonal selection, mutagenesis, and autocrine growth regulation by granulocyte colony-stimulating factor and granulocyte–macrophage colony-stimulating factor. *Am J Pathol* **159,** 1567–1579.

[20] Hubert P, van den Brûle F, Giannini SL, Franzen-Detrooz E, Boniver J, and Delvenne P (1999). Colonization of *in vitro*–formed cervical human papillomavirus–associated (pre)neoplastic lesions with dendritic cells: role of granulocyte/macrophage colony-stimulating factor. *Am J Pathol* **154,** 775–784.

[21] Skobe M, Rockwell P, Goldstein N, Vosseler S, and Fusenig NE (1997). Halting angiogenesis suppresses carcinoma cell invasion. *Nat Med* **3,** 1222–1227.

[22] Van Cauwenberge D, Pierard GE, Foidart JM, and Lapiere CM (1983). Immunohistochemical localization of laminin, type IV and type V collagen in basal cell carcinoma. *Br J Dermatol* **108,** 163–170.

[23] Bajou K, Masson V, Gerard RD, Schmitt PM, Albert V, Praus M, Lund LR, Frandsen TL, Brunner N, Dano K, et al. (2001). The plasminogen activator inhibitor PAI-1 controls *in vivo* tumor vascularization by interaction with proteases, not vitronectin. Implications for antiangiogenic strategies. *J Cell Biol* **152,** 777–784.

[24] Bajou K, Maillard C, Jost M, Lijnen RH, Gils A, Declerck P, Carmeliet P, Foidart JM, and Noel A (2004). Host-derived plasminogen activator inhibitor-1 (PAI-1) concentration is critical for *in vivo* tumoral angiogenesis and growth. *Oncogene* **23,** 6986–6990.

[25] Tomakidi P, Mirancea N, Fusenig NE, Herold-Mende C, Bosch FX, and Breitkreutz D (1999). Defects of basement membrane and hemidesmosome structure correlate with malignant phenotype and stromal interactions in HaCaT-Ras xenografts. *Differentiation* **64,** 263–275.

[26] Chan JC, Duszczyszyn DA, Castellino FJ, and Ploplis VA (2001). Accelerated skin wound healing in plasminogen activator inhibitor-1–deficient mice. *Am J Pathol* **159,** 1681–1688.

[27] Mueller MM and Fusenig NE (2002). Tumor–stroma interactions directing phenotype and progression of epithelial skin tumor cells. *Differentiation* **70,** 486–497.

[28] Czekay RP, Aertgeerts K, Curriden SA, and Loskutoff DJ (2003). Plasminogen activator inhibitor-1 detaches cells from extracellular matrices by inactivating integrins. *J Cell Biol* **160,** 781–791.

[29] Deng G, Curriden SA, Hu G, Czekay RP, and Loskutoff DJ (2001). Plasminogen activator inhibitor-1 regulates cell adhesion by binding to the somatomedin B domain of vitronectin. *J Cell Physiol* **189,** 23–33.

[30] Devy L, Blacher S, Grignet-Debrus C, Bajou K, Masson V, Gerard RD, Gils A, Carmeliet G, Carmeliet P, Declerck PJ, et al. (2002). The pro- or antiangiogenic effect of plasminogen activator inhibitor 1 is dose dependent. *FASEB J* **16,** 147–154.

[31] Lambert V, Munaut C, Noel A, Frankenne F, Bajou K, Gerard R, Carmeliet P, Defresne MP, Foidart JM, and Rakic JM (2001). Influence of plasminogen activator inhibitor type 1 on choroidal neovascularization. *FASEB J* **15,** 1021–1027.

[32] Lambert V, Munaut C, Carmeliet P, Gerard RD, Declerck PJ, Gils A, Claes C, Foidart JM, Noel A, and Rakic JM (2003). Dose-dependent modulation of choroidal neovascularization by plasminogen activator inhibitor type I: implications for clinical trials. *Invest Ophthalmol Vis Sci* **44,** 2791–2797.

[33] McMahon GA, Petitclerc E, Stefansson S, Smith E, Wong MK, Westrick RJ, Ginsburg D, Brooks PC, and Lawrence DA (2001). Plasminogen activator inhibitor-1 regulates tumor growth and angiogenesis. *J Biol Chem* **276,** 33964–33968.

[34] Stefansson S, Petitclerc E, Wong MK, McMahon GA, Brooks PC, and Lawrence DA (2001). Inhibition of angiogenesis *in vivo* by plasminogen activator inhibitor-1. *J Biol Chem* **276,** 8135–8141.

[35] Ploplis VA, Balsara R, Sandoval-Cooper MJ, Yin ZJ, Batten J, Modi N, Gadoua D, Donahue D, Martin JA, and Castellino FJ (2004). Enhanced *in vitro* proliferation of aortic endothelial cells from plasminogen activator inhibitor-1–deficient mice. *J Biol Chem* **279,** 6143–6151.

[36] Noel AC, Lefebvre O, Maquoi E, VanHoorde L, Chenard MP, Mareel M, Foidart JM, Basset P, and Rio MC (1996). Stromelysin-3 expression promotes tumor take in nude mice. *J Clin Invest* **97,** 1924–1930.

[37] Boulay A, Masson R, Chenard MP, El Fahime M, Cassard L, Bellocq JP, Sautes-Fridman C, Basset P, and Rio MC (2001). High cancer cell death in syngeneic tumors developed in host mice deficient for the stromelysin-3 matrix metalloproteinase. *Cancer Res* **61,** 2189–2193.

[38] Andarawewa KL, Boulay A, Masson R, Mathelin C, Stoll I, Tomasetto C, Chenard MP, Gintz M, Bellocq JP, and Rio MC (2003). Dual stromelysin-3 function during natural mouse mammary tumor virus-ras tumor progression. *Cancer Res* **63,** 5844–5849.